## 30.0 MICROSTRUCTURAL EVOLUTION OF METALLIC ALLOYS DURING RAPID SOLIDIFICATION (LEVERAGED)

Chloe Johnson (Mines)
Faculty: Amy Clarke (Mines)
Other Participants: Yaofeng Guo (Mines), J. Klemm-Toole (Mines), F.G. Coury (UFSCar), Joe McKeown (Lawrence Livermore National Laboratory)
Industrial Mentor: TBD (Los Alamos National Laboratory), TBD (Boeing)

This project initiated in Fall 2017 and is supported by the George S. Ansell Department of Metallurgical and Materials Engineering Fellowship and A.J. Clarke's startup funds at the Colorado School of Mines (Mines). The research performed during this project will serve as the basis for an Ph.D. thesis for Chloe Johnson.

### 30.1 Project Overview and Industrial Relevance

Understanding the relationship between processing, microstructure, and final performance of a metallic alloy is a fundamental goal of materials science. This begins with understanding the as-solidified microstructure of a metallic alloy, as this can greatly impact subsequent solid-state microstructural evolution and the final microstructure. While conventional solidification techniques have been extensively studied, far from equilibrium processes that involve rapid solidification (e.g. additive manufacturing, AM) are not entirely understood. Processes like AM result in unique grain morphologies and metastable phases that can change the expected final properties of a metallic component. Because of this, it is important to understand the mechanisms controlling microstructural development during far from equilibrium processing to help predict and optimize performance.

Although rapid solidification studies have been performed on some aluminum alloys, most have involved post mortem characterization of microstructures. Limited in-situ studies have been performed to date to observe rapid solidification of a few alloy systems [30.1-30.4]. This study proposes to use in-situ imaging techniques to understand microstructural development during rapid solidification of binary aluminum alloys (Al-Cu, Al-Ag, and Al-Ge). This will be coupled with ex-situ analyses to capture a range of solidification structures for different processing conditions. Aluminum alloy powders with ceramic inoculants will also be imaged during processing for the first time. Investigating the effect of rapid solidification conditions on microstructural development will provide new understanding about emerging technologies like AM.

### 30.2 Previous Work

In-situ rapid solidification studies have been performed on Al-Cu and Al-Si alloys using the Dynamic Transmission Electron Microscope (DTEM) at Lawrence Livermore National Laboratory (LLNL) [30.1-30.2]. This in-situ technique images the evolution of the melt-pool during rapid solidification, capturing the growth of microstructural features and allowing for the determination of solidification velocities as features develop. This technique has been used by our group to also image Al-Ge, mainly to further explore the development of the metastable monoclinic (M) phase and the metastable phase diagram proposed by Laoui and Kaufman, as shown in **Figure 30.1** [30.4]. The work of Laoui and Kaufman suggests that at compositions just below the solubility limit of the M phase (i.e. below 50.5 at. % Ge), the M phase is the primary phase, given sufficient undercooling. Above this limit, the M phase may form and re-melt in the liquid before the formation of the stable β phase. To try to capture this phenomenon, initial DTEM experiments were performed across a wide variety of compositions (46-76 at. % Ge). An initial study done by our group focused on identifying the phases in the two low-Ge compositions (46 and 58 at. % Ge) and the crystal structure of the M phase. The latter was done using a 46 at. % Ge alloy found to contain primary M phase dendrites. Formation and remelting of the M phase in the liquid, however, was not successfully captured in the dynamic data for the samples above 50.5 at. % Ge. Experiments are ongoing to further investigate this phenomenon.

Previous directional solidification studies performed by our group include Al-Ag alloys, which tends to exhibit significant solute segregation and coring during solidification. The goal of selecting Al-Ag alloys was to study homogenization and the role of chemical inhomogeneity on solid-state phase transformations. As a model system, Al-

Cu alloys were also selected to compare with previous rapid solidification studies and modeling [30.5] of microstructural evolution [30.1-30.2, 30.5-30.6].

## 30.3 Recent Progress

### 30.3.1 Rapid Solidification (DTEM) of Al-Ge

Recent studies with Al-Ge have focused on identification of phases in the remaining compositions (63-76 at. % Ge), as well as investigating microstructural trends and their correlation to local solidification and solute conditions. In previous work, it was found that the phases present in the 46 at. % Ge alloy were primary M phase dendrites surrounded by M + α eutectic, with some β phase particles between dendrites (**Figure 30.2**). The 58 at. % Ge alloy samples were found to contain primary β phase particles throughout the melt pool, with a transition zone near the edge containing secondary Al-rich dendrites surrounded by an Al-rich + Ge-rich coupled growth structure, and a region away from the edge containing only M + α eutectic surrounding the β phase particles (**Figure 30.3**). Recent studies have focused on 63, 64-66, and 70-76 at. % Ge samples. Both the 63 and 64-66 at. % Ge alloy samples show primary β phase particles surrounded by two different types of microstructures from melt pool to melt pool (**Figure 30.4**). Some melt pools are composed completely of β phase particles surrounded by Al-rich dendrites and eutectic, while others show this microstructure at the edge of the melt pool, with β phase particles surrounded entirely by eutectic away from the edge. Compositional analysis of the eutectic between the dendrites shows that the lighter areas are 22 at. % Ge, and the darker areas are 78 at. % Ge. This composition is inconsistent with the composition of the M phase (~43-45 at. % Ge) [30.7], which means this could be equilibrium α + β eutectic. This is currently being confirmed with electron diffraction. The eutectic away from the edge of the melt pool shows a similar morphology to the M + α eutectic observed in the 58 at. % Ge alloy sample. The 70-76 at. % Ge alloy samples are composed of large β phase particles surrounded by eutectic (**Figure 30.5**). Electron diffraction still needs to be performed to confirm the phases compromising these latter two eutectics. So far, these observations are consistent with the findings of Laoui and Kaufman [30.4].

The observed transition regions where the microstructure surrounding the primary phase transitions from a region of Al-rich dendrites and eutectic to a region of purely eutectic can be explained based on local solute and undercooling conditions. Near the edge of the melt pool, the volume fraction of β phase particles appears to be larger, leading to a higher local concentration of Al solute rejected into the liquid as these particles form. The Al concentration in the liquid is high enough to form Al-rich dendrites around these particles, and the remaining liquid is Al poor to the point where there is not a high enough constitutional undercooling to form a metastable M + α eutectic. However, away from the edge of the melt pool, the volume fraction of β particles is lower. This leads to a lower concentration of Al in the liquid, as there is more liquid to distribute the solute. In this case, there is not enough Al solute for Al-rich dendrites to form; thus, the constitutional undercooling is high enough to form a metastable eutectic in certain compositions. At lower Ge compositions (58 at. % Ge) and higher compositions (up to 70-76 at. % Ge), this transition/dendritic region is smaller or almost negligible (**Figure 30.3**), whereas at intermediate compositions (63-66 at. % Ge), it is possible to see a microstructure consisting of this dendritic region (**Figure 30.4**). Phase fraction amounts are currently being evaluated to compare with undercooling predictions to confirm this hypothesis. So far, early results appear to be consistent. The difference in volume fraction could be related to β nucleation sites. These particles typically form anywhere in the melt pool, with a higher fraction at the edges, due to the higher initial heat extraction. Further investigation needs to be performed to see what factors, if any, could be affecting the volume fraction of β phase particles forming.

### 30.3.2 Current Rapid Solidification Experiments on Al-Ag

In-situ rapid solidification studies on Al-Ag are underway and are currently being studied post mortem. Initial and on-going studies were/are being performed with DTEM. More recently, an AM simulator at Argonne National Laboratory's (ANL) Advanced Photon Source (APS) was used to observe in-situ rapid solidification relevant to AM. Post mortem microstructural examinations and dynamic data will be presented in future reports.

### 30.3.3 Initial Characterization of Al 6061 MMC Powder & AM Build

Another focus of this project is to study the effect of inoculants on grain growth and selection during rapid solidification of ceramic particle-containing aluminum alloy powders. Initial characterization of the powder and AM builds of an Al 6061 MMC alloy has been performed using scanning electron microscopy (SEM) and electron dispersive spectroscopy (EDS). From SEM images of the powder, the particles were measured to be on the order of tens of microns (**Figure 30.6)**. An initial EDS scan showed the distribution of solute due to the reactions between the inoculant powder and the surrounding matrix (**Figure 30.7**). More work needs to be done to reveal and analyze the grain structure in these builds. In-situ studies using the AM simulator at APS have been performed on these alloys, both on AM built plates and AM built plates with powder, with post mortem analysis currently underway.

## 30.4 Plans for Next Reporting Period

- Identify phases in eutectics for various Al-Ge compositions;
- Investigate possible re-melting of the M phase for higher (> 50.5 wt.% Ge) Al-Ge alloy compositions via additional DTEM experiments;
- Correlate results extracted from image processing (e.g. phase volume fractions) to local microstructure evolution in Al-Ge melt pools;
- Analyze early DTEM experiments on Al-Ag alloys;
- Analyze recently collected APS data of Al-Ag alloys and a Al 6061 MMC alloy;
- Post-mortem characterization of Al-Ag and Al 6061 MMC AM builds.

## 30.5 References

[30.1] J. McKeown, K. Zweiacker, C. Liu, D.R. Coughlin, A.J. Clarke, J.K. Baldwin, J.W. Gibbs, J.D. Roehling, S.D. Imhoff, P.J. Gibbs, D. Tourret, J.M.K. Wiezorek, G.H. Campbell, "Time-resolved in situ measurements during rapid alloy solidification: experimental insight for additive manufacturing", JOM, 2016, 68(3):985-999

[30.2] J. McKeown, A. Kulovits, C. Liu, K. Zweiacker, B. W. Reed, T. LaGrange, J.M.K. Wiezorek, G.H. Campbell, "In situ transmission electron microscopy of crystal growth-mode transitions during rapid solidification of a hypoeutectic Al-Cu alloy", Acta Materialia, 2014, 65:56-68

[30.3] C. Zhao, K. Fezzaa, R. Cunningham, H. Wen, F. De Carlo, L. Chen, A.D. Rollett, T. Sun, "Real-time monitoring of laser powder bed fusion process using high-speed X-ray imaging and diffraction", Scientific Reports, 2017, 7:3602

[30.4] T. Laoui and M. Kaufman, "Nonequilibrium behavior in the Al-Ge alloy system: insights into the metastable phase diagram", Metallurgical and Materials Transactions A, 1991, 22(9):2141-2152

[30.5] T.T. Roehling, S.S. Q. Wu, S.A. Khairallah, J.D. Roehling, S.S. Soezeri, M.F. Crumb, M.J. Matthews, "Modeling laser intensity profile ellipticity for microstructural control during metal additive manufacturing" Acta Materialia, 2017, 128:197-206

[30.6] D. Tourret, J.C.E. Mertens, E. Lieberman, S.D. Imhoff, J.W. Gibbs, K. Henderson, K. Fezzaa, A.L. Deriy, T. Sun, R.A. Lebensohn, B.M. Patterson, A.J. Clarke, "From solidification processing to microstructure to mechanical properties: a multi-scale x-ray study of an Al-Cu alloy sample", Metallurgical and Materials Transactions A, 2017, 48(11):5529-5546

[30.7] M. Kaufman, J. Cunningham, H. Fraser, "Metastable phase production and transformation in Al-Ge alloy films by rapid crystallization and annealing treatments", Acta Metallurgica, 1987, 35(5):1181-1192

## 30.6 Figures and Tables

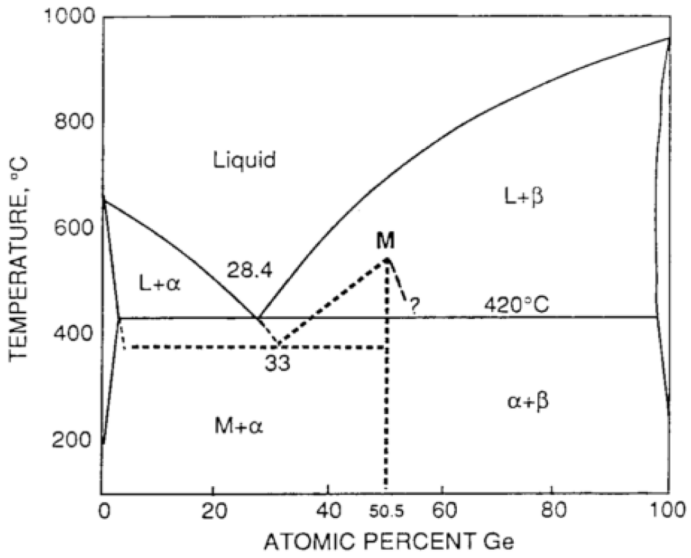


Figure 30.1: Al-Ge phase diagram, showing the proposed metastable phase diagram for the metastable monoclinic (M) phase [30.4].

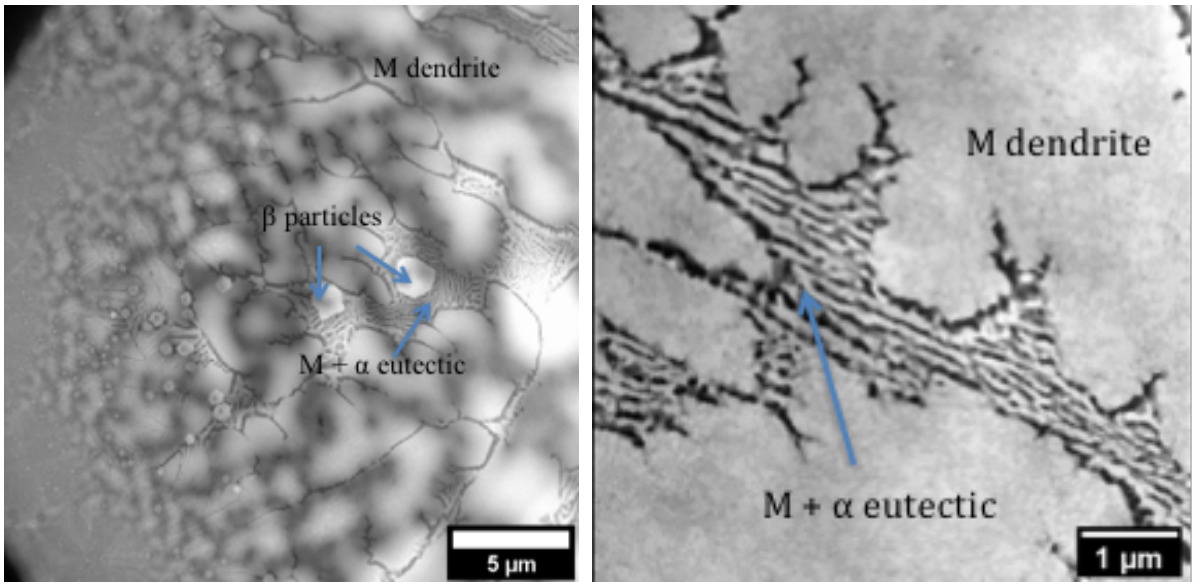


Figure 30.2: Post-mortem TEM images of DTEM generated melt pools in the 46 at. % Ge alloy samples. A) a melt pool containing M phase dendrites, β particles, and M + α eutectic. B) a higher magnification image of M phase dendrites and M + α eutectic. Courtesy of F.G. Coury, Mines.

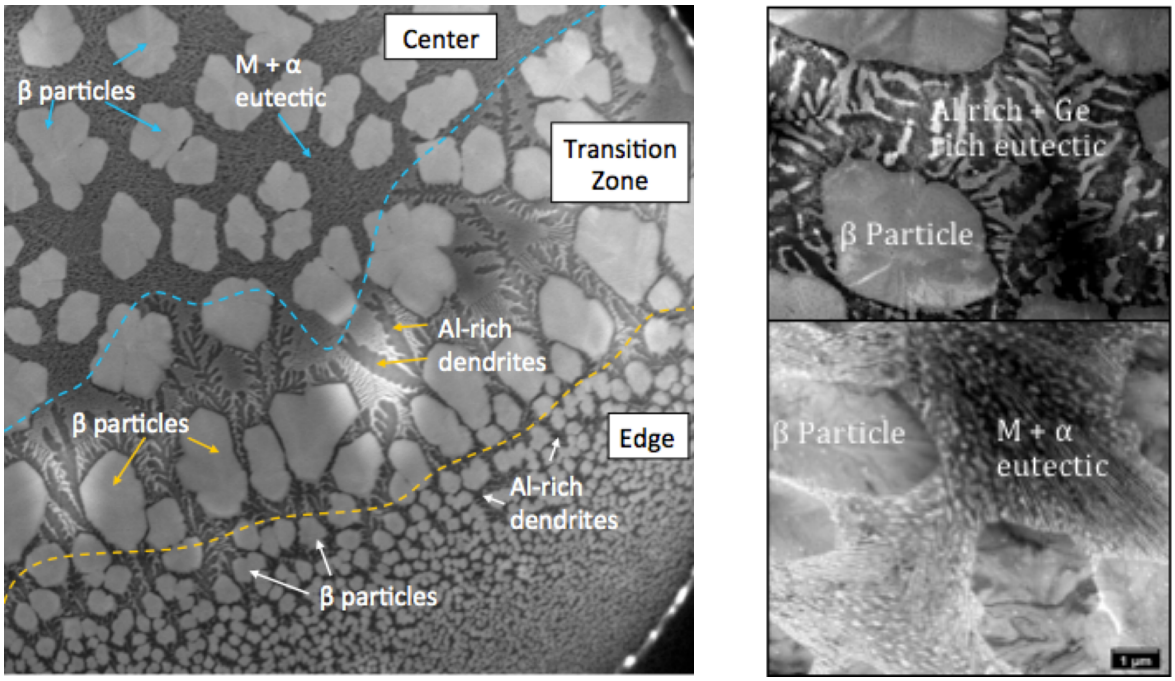


Figure 30.3: Post-mortem TEM images of DTEM generated melt pools in the 58 at. % Ge alloy samples. A) A melt pool containing primary β particles, surrounded by various microstructures (labeled above). B) A higher magnification image of the Al-rich and Ge-rich eutectic surrounding the β particles in the transition zone (labeled above). C) A higher magnification image of the M + α eutectic surrounding β particles in the center region of the melt pool (labeled above). Courtesy of F.G. Coury, Mines.

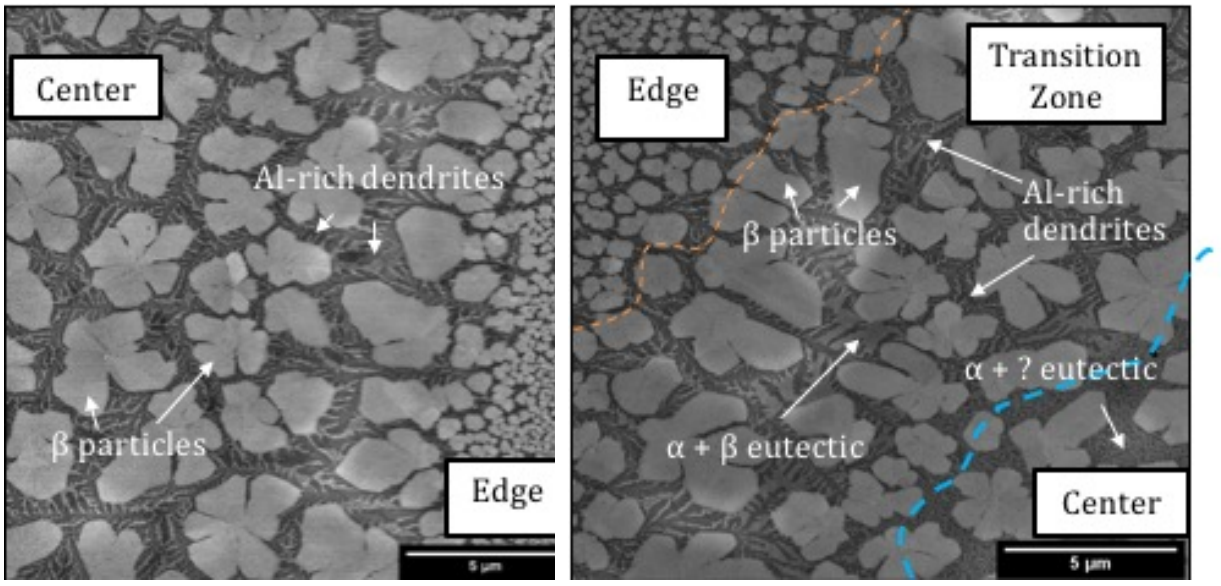


Figure 30.4: Post-mortem TEM images of DTEM generated melt pools in the 63-66 at. % Ge alloy samples. A) A melt pool containing β particles, surrounded by Al-rich dendrites and eutectic. B) a melt pool containing β particles with a region surrounded by Al-rich dendrites and eutectic, as well as a region surrounded by an unidentified eutectic. Courtesy of Y. Guo, Mines.

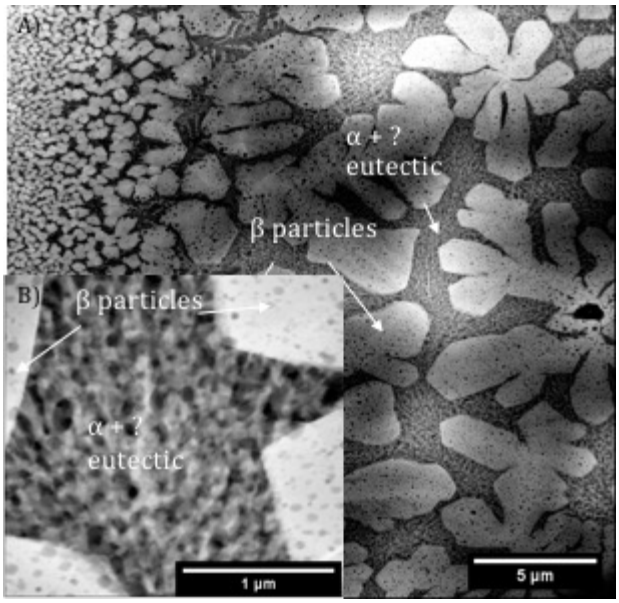


Figure 30.5: Post-mortem TEM images of DTEM generated melt pools in the 70-76 at. % Ge alloy samples. A) A melt pool containing β particles, surrounded by an unidentified eutectic. B) A higher magnification of this surrounding eutectic. Courtesy of Y. Guo, Mines.

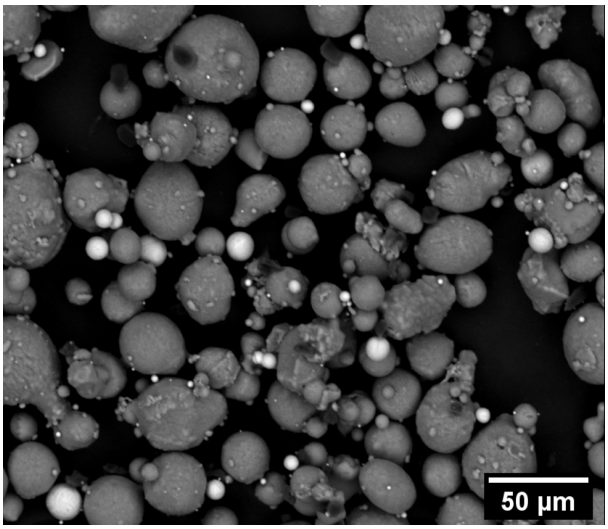


Figure 30.6: SEM image of the Al 6061 MMC powder. The white particles are innoculants and the grey particles are the Al 6061 alloy powder.

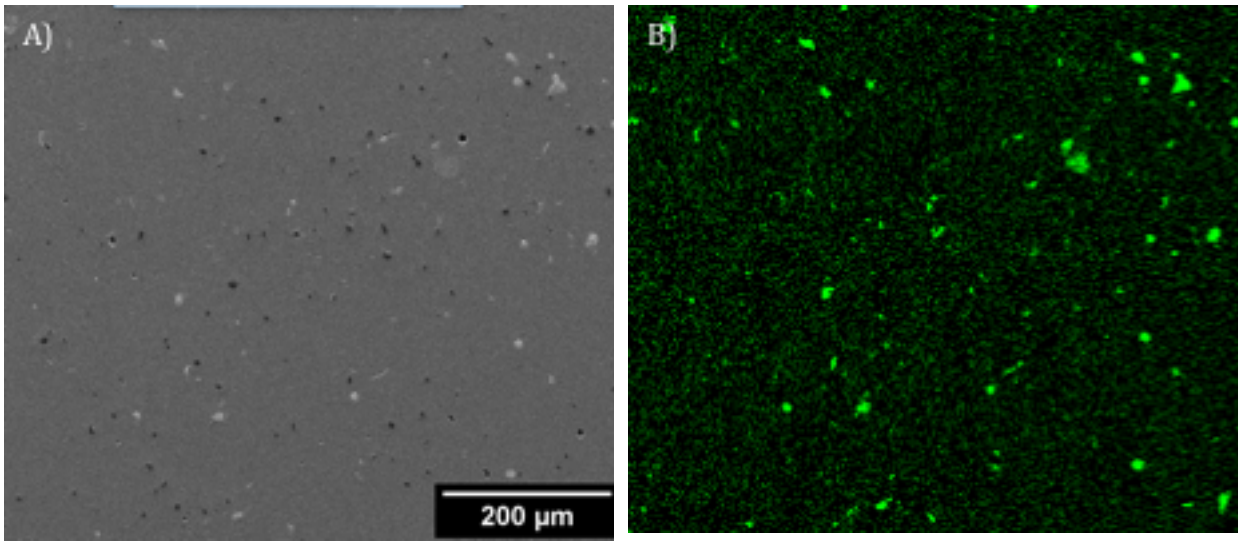


Figure 30.7: A) SEM image of the Al 6061 MMC AM build. B) EDS scan showing the solute distribution from the reaction between the inoculant powder and the Al 6061 matrix during the AM process.